engineering proceedings

MDPI

Proceeding Paper

Temperature dependent dielectric studies of Copper and Magnesium doped Zinc aluminate: Implications for electrical Behavior†

Yasmin Jamil, Gracie.P. Jeyakumar and Geetha Deivasigamani *

Department of Applied Sciences and Humanities, MIT, Anna University, Chennai-44, India

* Correspondence: geetha@mitindia.edu.

† Presented at the 4th International Electronic Conference on Applied Sciences (ASEC 2023), 27 October-10 November.

Abstract: Copper (Cu^{2+}) and magnesium (Mg^{2+})-doped Zinc aluminate $ZnAl_2O_4$ is a promising material with diverse applications in electronic and energy storage devices. In this study, synthesis of $Zn_{0.9}M_xAl_2O_4$ (M= Cu^{2+}&Mg^{2+}; x=0.00 and 0.10) has been conducted via sol–gel combined combustion technique. The structural, spectral, optical and dielectric parameters of the synthesized spinel aluminates were analysed to explore the substitution effect of Cu^{2+} and Mg^{2+} content. The formation and crystallinity analysis of single-phase cubic spinel structure in synthesized spinel aluminates were confirmed using XRD patterns. The lattice parameter and grain size were ascertained from the XRD data. Crystallite size of Cu^{2+} and Mg^{2+} substituted $ZnAl_2O_4$ using the Scherrer's formula was found to be around 22 nm. Spinel structure formation in prepared spinel aluminates were ascertained by FT-IR study. The UV-Vis spectra exhibited a broad absorption band in the UV-Vis region, indicating the presence of electronic transitions. The bandgap energy of the prepared aluminates was estimated from the absorption edge with values varying between 2.90 eV to 3.03 eV, revealing its suitability for optoelectronic applications. Measurement of dielectric parameters were performed in the frequency range of 100 Hz to 20 MHz at temperatures ranging from 30°C to 250°C. The dielectric constant (ε') and dielectric loss (ε'') were determined as a function of frequency at different temperatures. The results showed that the dielectric constant decreased with increasing frequency for all the observed temperatures, while the dielectric loss exhibited a peak at a specific temperature. The conductivity results indicates that the conduction mechanism occurred due to polaron hopping. Arrhenius relation was adopted to calculate the activation energies E_a for all the samples and the values were between 0.70 eV to 0.38 eV. The obtained results were discussed and interpreted. These findings contribute to the understanding of the electrical behaviour of doped zinc aluminate materials and their useful applications in different electronic and energy systems.

Keywords: Combustion method; Band-gap; Maxwell-Wagner; Ac conductivity

Citation: To be added by editorial staff during production.

Academic Editor: Firstname Lastname

Published: date

Copyright: © 2023 by the authors. Submitted for possible open access publication under the terms and conditions of the Creative Commons Attribution (CC BY) license (https://creativecommons.org/licenses/by/4.0/).

1. Introduction

Spinel $ZnAl_2O_4$ are a class of fascinating materials that exhibit intriguing and versatile applications due to their unique crystal structure and composition. The semiconductor $ZnAl_2O_4$ has fascinating characteristics that make it suitable for broad technological applications like sensors, photocatalysts, microwave devices, ceramic pigments and microelectronics. Also, due to its remarkable properties like high melting point and large surface area, it is widely studied for high temperature fuel cells, dielectric materials and for other optoelectronic applications [1, 2]. Substitution or doping of transition metal ions into the aluminates system results in enhancement of optical and electrical properties. The aim of current research is : (i) to improve the properties by

bringing down the dimension to nanosize and (ii) to observe the effects of substitution on structural, optical and dielectric properties. Earlier studies on nanocrystalline $ZnAl_2O_4$ had reported low dielectric constant, better conductivity and enhanced optical property [3]. Various synthesis routes have been adopted to synthesize spinel aluminates like cost effective sol-gel auto combustion method, co precipitation method, mixed oxide method and microwave method. Out of all these methods sol-gel auto combustion method is the most reliable and cost-effective method to synthesize spinel aluminates. Hence simple sol gel auto combustion method was adopted to synthesize single phase $Zn_{1-x}Cu_xAl_2O4$ and $Zn_{1-x}Mg_xAl_2O_4$ (x=0.0 and 0.1). We have discussed the effects of Cu and Mg substitution on $ZnAl_2O_4$ and their structural, optical and dielectric properties are discussed in detail.

2. Materials and Methods

The nitrate precursors in the form of zinc $Zn(NO_3)_2.6H_2O$, aluminium $Al(NO_3)_2.9H_2O$, cupric $Cu(NO_3)_2.3H_2O$, magnesium Mg $(NO_3)_2$ $.6H_2O$ were taken for the preparation of spinel aluminates. Citric acid monohydrate ($C_6H_8O_7.H_2O$) as chelating agent, distilled water H_2O as solvent and ammonia solution to balance the pH= 9 was used. Stoichiometric ratios of $Zn(NO_3)_2.6H_2O$, $Al(NO_3)_2.9H_2O$ and $C_6H_8O_7.H_2O$ in the ratio of 1:2:2 was dissolved in sufficient amount of distilled water and the solution was magnetically stirred for 2 hours at room temperature. Ammonia solution was added dropwise until the desired pH was reached. The temperature was then gradually increased after 2 hours for gelation. The obtained gel was combusted at 100℃ and the powders were calcined at 800℃ for 3 hours. For Cu and Mg substituted samples the same procedure was adopted by adding the Cu and Mg derivatives into the solution. The samples were then named as ZnAl, ZnAl:Cu and ZnAl:Mg. The obtained aluminate powders were utilized for further characterizations.

The phase and crystalline structure were characterized by X-ray diffraction technique (XRD: D8 Advance Bruker AXS, Germany). Functional groups in the 400-4000cm^{-1} range spectra was used to compute the designated transmittance bands using Fourier-transform infrared (FTIR- Shimadzu). The optical spectra analysis was done by UV-DRS spectroscopy (SHIMADZU UV-1800 JAPAN). Broadband dielectric spectroscopy BDS(NOVOCONTROL) was used to record the dielectric parameters in the frequency range of 100Hz-20MHz at temperatures ranging from room temperature to 250 ℃.

3. Results and Discussion

3.1. Structural Properties-XRD

The diffraction patterns of ZnAl, ZnAl:Cu and ZnAl:Mg shown in Fig. 1, were estimated using X-ray diffraction method. The XRD patterns ensure the formation of uni-phase spinel cubic structure of the prepared aluminates. The obtained patterns were indexed with Miller indices (111), (2 2 0), (3 1 1), (4 0 0), (331), (4 2 2), (5 1 1), (4 4 0), (620) and (533) associated to the various planes and the observed results was in correlation with JCPDS card No: 05-0669 and earlier reported literature [4].

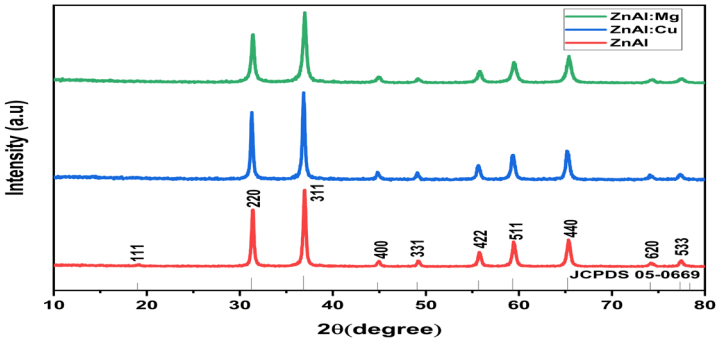

Figure 1. XRD patterns of ZnAl, ZnAl:Cu and ZnAl:Mg.

The lattice parameter (a) was obtained for the high intense peak (311) using the Nelson and Rilay relation:

$$f(\theta) = \frac{1}{2}\left(\frac{cos^2\theta}{sin\theta} + \frac{cos^2\theta}{\theta}\right) \quad (1)$$

Where θ is the angle of diffraction. The lattice parameters of ZnAl:Cu and ZnAl:Mg are lesser than the parent ZnAl which may be due to ionic radii of the substituted cation reordering with the cubic spinel phase. The volume of the unit cell was calculated using $V= a^3$ and the crystallite size(D) was calculated by employing Scherrer's formula which is given by

$$D = \frac{k\lambda}{\beta cos\theta} \quad (2)$$

Where k is shape factor whose value is 0.9, λ is the wavelength of Cu-Kα source, β is the full width half maxima FWHM and θ is the diffraction angle. The average crystallite size and structural parameters calculated from XRD patterns are shown in Table 1.

Samples	Crystallite size D(nm)	Lattice parameter a(A°)	Dislocation density δ	Volume of the unit cell $V=a^3$(A°)
ZnAl	22.818	8.0815	1.9205	527.69
ZnAl:Cu	23.048	8.0564	1.8823	523.54
ZnAl:Mg	22.920	8.0575	1.9034	523.56

Table 1. Structural parameters of ZnAl, ZnAl:Cu and ZnAl:Mg.

3.2. FT-IR Analysis

FT-IR patters of ZnAl, ZnAl:Cu and ZnAl:Mg are shown in Fig. 2. The assurance of the spinel structure was confirmed from the transmittance bands present in the fingerprint region 450 cm^{-1} to 790 cm^{-1}. The occurrence of transmittance bands at 661.53 cm^{-1} is associated to vibration of Zn-O, the band at 554.49 cm^{-1} is associated to vibration of Al-O and the band at 496.63 cm^{-1} can be associated to the vibration of Zn-O-Al at tetrahedral and octahedral sites respectively. The aluminate samples also contain another transmittance bands around 2354.27 cm^{-1} and 3437.87cm^{-1} which are associated to CO_2 bands and -O-H stretching band respectively. The other bands at 1627 cm^{-1} and 1408 cm^{-1} are assigned to the symmetric and asymmetric vibrations of C-H [5]. The intensity of the transmittance bands gets broader and shorter due to substitution of Cu and Mg in the zinc site and due to the ionic radii of the substitution ion.

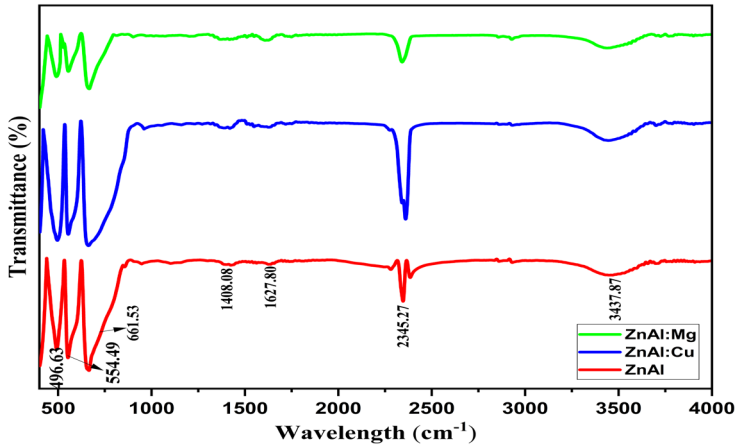

Figure 2. FT-IR spectra of ZnAl, ZnAl:Cu and ZnAl:Mg.

3.3. UV-DRS Analysis.

The optical energy band gap of ZnAl, ZnAl:Cu and ZnAl:Mg recorded in the range of 200nm -800 nm using UV-DRS technique are shown in Fig. 3. Strong absorption peaks for all the aluminates were observed in the visible region of the spectra. The band gap energy was calculated using the Tauc's relation given by

$$(\alpha h\nu)^n = A(h\nu - E_g) \quad (3)$$

where α is the absorption coefficient, hν is the photon energy, A is a constant depending on the type of transition and n is the coefficient of allowed transitions. For direct band gap $n = 1/2$ and for indirect band n=2. By finding the intercept on the hν axis and extrapolating the plot $(\alpha h\nu) = 0$, the band gap can be estimated [6,7]. The optical direct band gap energy of ZnAl, ZnAl:Cu and ZnAl:Mg were 3.03 eV, 2.94 eV and 2.90 eV respectively. As seen from the Fig. 3, the band gap energy of Cu and Mg doped aluminates was found to decrease compared to the parent sample. This may be due to the quantum confinement effect owing to small crystallite size of prepared aluminates [3].

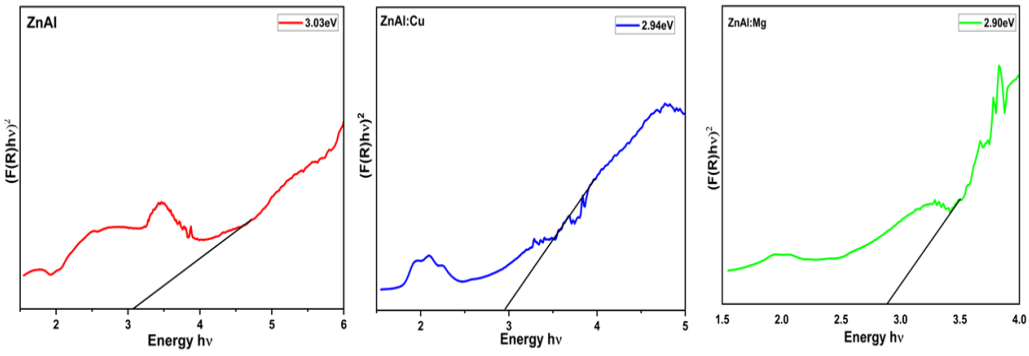

Figure 3. Tauc's plots of ZnAl, ZnAl:Cu and ZnAl:Mg.

3.4. Temperature dependent Dielectric parameters

3.4.1. Dielectric Studies: Dielectric constant ε', tangent loss tan δ and AC conductivity σ_{ac}

The real and imaginary part of dielectric constant ε' is expressed in terms of complex permittivity given below:

$$\varepsilon'(\omega) = \varepsilon_\infty + \frac{\varepsilon_s - \varepsilon_\infty}{1 + \omega^2\tau^2} \quad (4)$$

$$\varepsilon''(\omega) = \varepsilon_s - \varepsilon_\infty + \frac{\omega\tau}{1 + \omega^2\tau^2} \quad (5)$$

Where ε_∞ is the permittivity at higher frequency limit, ε_s is the static, low frequency permittivity and τ is the characteristic relaxation time of the medium. The above two equations are known as Debye equations. Equation (4) gives a clear understanding about the decline in dielectric constant ε′ with increase in frequency. Fig. 4(A-C) represents the dielectric constant ε′ of ZnAl, ZnAl:Cu and ZnAl:Mg as a function of frequency ranging from 100Hz to 20MHz at temperatures 303K- 523K. It can be observed that dielectric constant is very high at lower frequency domain and as it approaches higher frequency the dielectric constant ε′ achieves minimum value or becomes constant. This dispersive nature of dielectric constant ε′ can be explained by Maxwell-Wagner type interfacial polarization as suggested by Koop's model which states that at low frequencies region the charge carriers have the tendency to follow the applied electric field whereas at high frequencies region the charge carriers lag the applied electric field which results in decline of the dielectric constant ε′ [8, 9]. It is known that the grain boundaries are primarily composed of O_2 and non-stoichiometric dangling bonds which functions as electron trap within the system. On applying the electric field, the mobile electrons move towards the grain boundary through the conductive path's grains facilitated by the dangling bonds present. Owing to high resistance at grain boundary, the mobile electrons gather there resulting in elevated dielectric values at lower frequencies. Whereas as applied field increases, a significant portion of the electrons lose their capability to respond to the electric field applied and consequently change direction more rapidly making it difficult to reach the grain boundaries and substantially the dielectric constant ε′ decreases at higher frequency region [10,11]. We can also see that as temperature increases the dielectric constant decreases ε′ at low frequency for all the temperatures as a result of thermal activation and accommodates more charges at grain boundaries. However, it reaches a minimum value at higher frequencies for all the observed temperatures. The composition dependence of dielectric constant can be explained based on electron exchange between $Al^{2+} \leftrightarrow Al^{3+}$ octahedral sites and polaron hopping of electrons [11]. When Cu and Mg is substituted into the parent material at Zn site the dielectric constant ε′ decreases because Cu and Mg have more probability to accommodate at B-site ions. As a result of this there is a reduction in the concentration of aluminium ions at octahedral sites which ruptures the charge transfer between $Al^{2+} \leftrightarrow Al^{3+}$ and this effects the polarization mechanism.

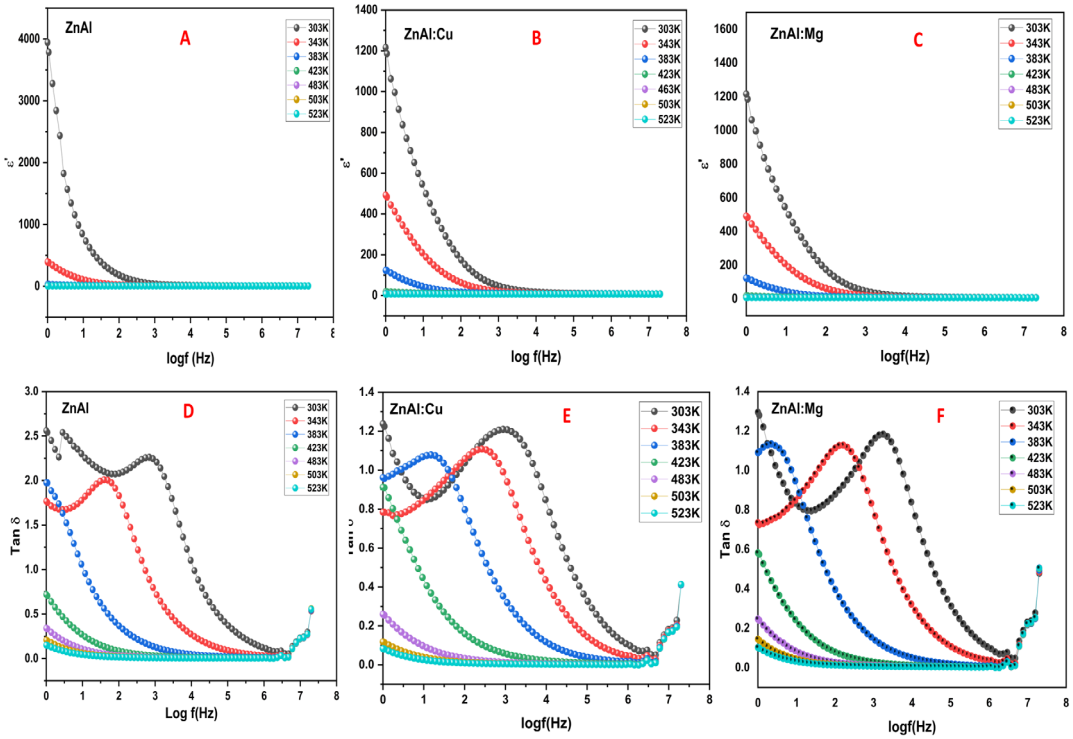

Figure 4. Dielectric constant ε′ (A-C) and Tangent loss Tanδ (D-F) of ZnAl, ZnAl:Cu and ZnAl:Mg Vs frequency at several temperatures.

Fig. 4 (D-F) represents the tangent loss tanδ of ZnAl, ZnAl:Cu and ZnAl:Mg as a function of frequency ranging from 100Hz to 20MHz at temperatures 303K-523K. The tangent loss is given by

$$\tan\delta = \frac{\varepsilon''}{\varepsilon'} \tag{6}$$

At lower frequency region, tan δ increases and as frequency increases the loss decreases . Each sample shows some extra-ordinary behavior at lower frequency region at specific temperatures. The presence of relaxation peak in the curve at lower frequency region indicates that the dielectric constant contribution is large to the variation of tan δ and due to the accumulation of charge carriers at low temperatures and frequency [3,9]. The hopping of electrons at low frequency needs sufficient energy due to resistive nature of grain and grain boundary which results in high value of tan δ. Higher the frequency there is minimum electron hopping because the resistive nature of grain boundaries decreases and energy consumption is less. Also, there are sometimes additional losses which may be due to disorders in the crystal system and imperfections. As the temperature decreases the values of tangent loss decreases and these results are related to previous literatures. The tangent loss has the least value for the Cu and Mg substituted samples compared with parent sample.

3.4.1. Ac Conductivity.

The ac conductivity σ_{ac} of ZnAl, ZnAl:Cu and ZnAl:Mg as a function of frequency ranging from 100 Hz to 20 MHz at temperatures 303 K- 523 K is displayed in Fig. 5. From the ac conductivity plot it is seen that as frequency increases the conductivity also increases at all the given temperatures for all the samples and the values of conductivity are larger in higher frequency regions due to polaron hopping present in sample [8, 9]. The frequency and temperature dependent conductivity is closely associated to universal Jonscher's power law given by the relation

$$\sigma_t = \sigma_{dc} + A\omega^n \quad (7)$$

Where σt is the total conductivity, σ_{dc} is the dc conductivity and temperature dependent, ω is the angular frequency $\omega = 2\pi f$, A is coefficient and n is the frequency exponent dependent on temperature. Jonscher's power law is obtained by plotting ln(σ_{ac}) as a function of logarithmic frequency as shown in Fig. 5.

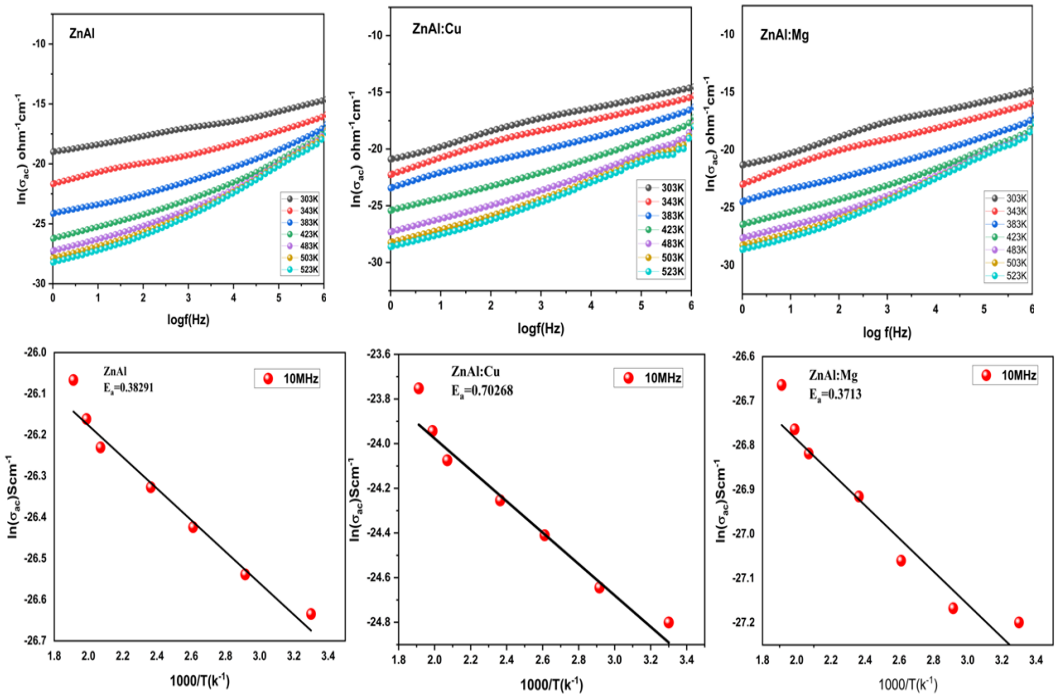

Figure 5. AC conductivity plots of of ZnAl, ZnAl:Cu and ZnAl:Mg at various temperatures and Arrhenius plots of ZnAl, ZnAl:Cu and ZnAl:Mg at 10 MHz.

The relation between ac conductivity σ_{ac}, real dielectric constant ε, frequency, and dielectric loss can be expressed as

$$\sigma_{ac} = \varepsilon' \varepsilon_0 \omega \tan\delta \quad (8)$$

The dielectric structure of spinel systems consists of two layers i.e., conducting grains and non-conducting grain boundaries. On applying the field, the long-range inter well hopping of holes between $Al^{2+} \leftrightarrow Al^{3+}$ sites located near defect-potential wells or a short range intrawell hopping within one defect-potential well may occur [3,12]. The dc part of the total conductivity contributes to inter-well hopping while ac conductivity to intrawell hopping. Hence a gradual increase in ac conductivity with frequency is observed. Using the temperature dependent ac and dc conductivity, the activation energy can be calculated using the Arrhenius relation given by

$$\sigma_{ac} = \sigma_o exp \frac{-E_a}{k_B T} \quad (9)$$

where, σ_o is the pre-exponential factor, Boltzmann's constant with temperature (K_BT) and E is the activation energy of the sample. The plot of log(σ_{ac}) vs. 1000/T, is shown in Fig. 5. The activation energies of ZnAl, ZnAl:Cu and ZnAl:Mg for 10MHz were found to vary between 0.70eV to 0.38 eV.

4. Conclusion

A simple sol -gel combustion method was used to prepare spinel Cu and Mg substituted zinc aluminates. XRD patterns confirmed the single phase formation of synthesized aluminates with an average crystallite size varying between 22.6 nm to 23.05 nm. The characteristic transmittance bands in the finger print region confirms the spinel structure of the aluminates. The optical spectra indicated a decrease in band gap of the aluminates and the values were found to be 3.03 eV, 2.90 eV and 2.94 eV for ZnAl, ZnAl:Cu and ZnAl:Mg respectively. The dielectric constant ε′ and tangent loss tan δ values of synthesized zinc aluminates decreased substantially at higher frequencies for all the observed temperatures obeying Maxwell-Wagner interfacial polarization. The AC conductivity σ_{ac} spectra of the synthesized zinc aluminates as a function of frequency at several temperatures was investigated and the conductivity increased as the frequency increased. The conductivity mechanism was discussed in detail based on grain and grain boundary contribution and hopping mechanism. The activation energies of the synthesized zinc aluminates were calculated using the Arrhenius relation and the values were between 0.70 eV to 0.38 eV. The activation energy E_a of ZnAl:Cu was found to be the highest. From the observed results, it can be propounded that the synthesized aluminates could be used for high frequency applications and memory-based storage devices.

Author Contributions: Conceptualization, Y.J.; methodology, Y.J.; software, Y.J.; validation, Y.J., G.P.J and G.D.; formal analysis, Y.J.; investigation, Y.J.; data curation, Y.J and G.P.J.; writing—original draft preparation, Y.J.; writing—review and editing, Y.J.; visualization, G.D and Y.J.; supervision, G.D.; project administration, G.D. All authors have read and agreed to the published version of the manuscript.

Funding: This research was funded by Anna centenary Research Fellowship ACRF, Anna university with Ref No: CFR/ACRF-2022/AR1.

Institutional Review Board Statement: Not applicable.

Informed Consent Statement: Not applicable.

Acknowledgments: Author Yasmin J; gratefully acknowledges Anna University, Chennai for providing ACRF Fellowship to carry out this research work.

Conflicts of Interest: The authors declare no conflict of interest.

References

1. New fuel governed combustion synthesis and improved luminescence in nanocrystalline Cr^{3+} doped $ZnAl_2O_4$ particles _ Elsevier Enhanced Reader. .
2. Jamil Y, Jeyakumar GP, Deivasigamani G. Investigation of Transition Metal Ions Cu^{2+} and Mg^{2+} Doped Zinc Aluminate ($ZnAl_2O_4$) and Their Structural, Spectral, Optical, and Dielectric Study for High-Frequency Applications. MDPI AG 2023, 2.
3. Muhammad E, Jamal A, Kumar S, Anantharaman MR. On structural, optical and dielectric properties of zinc aluminate nanoparticles. 2011.
4. Han M, Wang Z, Xu Y *et al.* Physical properties of $MgAl_2O_4$, $CoAl_2O_4$, $NiAl_2O_4$, $CuAl_2O_4$, and $ZnAl_2O_4$ spinels synthesized by a solution combustion method. Mater Chem Phys 2018; 215: 251–258.
5. Lu Q, Wei Z, Wu X, Huang S, Ding M, Ma J. Electronic structure and optical properties of spinel structure $Zn_{1-x}Ni_xAl_2O_4$ nanopowders synthesized by sol–gel method. Chem Phys Lett 2021; 772.
6. Priya A S, Geetha D. Impact of (Zr, Cu) ion substitution on the optical, dielectric, and impedance behavior of BiFeO3. Brazilian J Phy 2021; 51: 40-46.
7. Elakkiya V, Agarwal Y, Sumathi S. Photocatalytic activity of divalent ion (copper, zinc and magnesium) doped $NiAl_2O_4$. Solid State Sci 2018; 82: 92–98.
8. Rajamoorthy M, Geetha D, Sathiya Priya A. Synthesis of Cobalt-Doped $Bi_{12}NiO_{19}$: Structural, Morphological, Dielectric and Magnetic Properties. Arabian J Sci Engg 2021; 46: 737-744.
9. Saleem M, Varshney D. Influence of transition metal Cr^{2+} doping on structural, electrical and optical properties of Mg-Zn aluminates. J Alloys Compd 2017; 708: 397–403.

10. Priya AS, Geetha D. Studies on the multiferroic properties and impedance analysis of (La, Cu) $BiFeO_3$ prepared by sol-gel method. Ferroelectrics 2021; 573: 104-116
11. Samkaria R, Sharma V. Effect of rare earth yttrium substitution on the structural, dielectric and electrical properties of nanosized nickel aluminate. Solid State Mater Adv Technol 2013; 178: 1410–1415.
12. Mahmood A, Maqsood A. Temperature and frequency-dependent electrical transport studies of manganese-doped zinc ferrite nanoparticles. Mater Sci Eng B 2023; 296.

Disclaimer/Publisher's Note: The statements, opinions and data contained in all publications are solely those of the individual author(s) and contributor(s) and not of MDPI and/or the editor(s). MDPI and/or the editor(s) disclaim responsibility for any injury to people or property resulting from any ideas, methods, instructions or products referred to in the content.